Electronic Supplementary Information for:

Segregative Phase Separation of Strong Polyelectrolyte Complexes at High Salt and High Polymer Concentrations

Conner H. Chee, Rotem Benharush, Lexi R. Knight, and Jennifer E. Laaser*

S1 Supplemental Results

S1.1 Phase Behavior

Larger photographs of all phase-separated samples shown in Fib. 2(b) of the main text are included in Figure S1.

S1.2 Thermogravimetric Analysis

As discussed in the main text, the phase behavior of samples in both the normal binodal regime and the UPW was quantified by thermogravimetric analysis. Full TGA traces for samples prepared below the binodal are shown in Figure S2, and traces for samples prepared in the UPW are shown in Figure S3. As in the representative TGA traces shown in the main text, all samples prepared under the binodal exhibited distinct polymer-rich and polymer-poor phases, while samples prepared in the UPW had substantial salt and polymer content in both phases.

*Department of Chemistry, University of Pittsburgh, 219 Parkman Ave, Pittsburgh, PA, USA. E-mail: j.laaser@pitt.edu

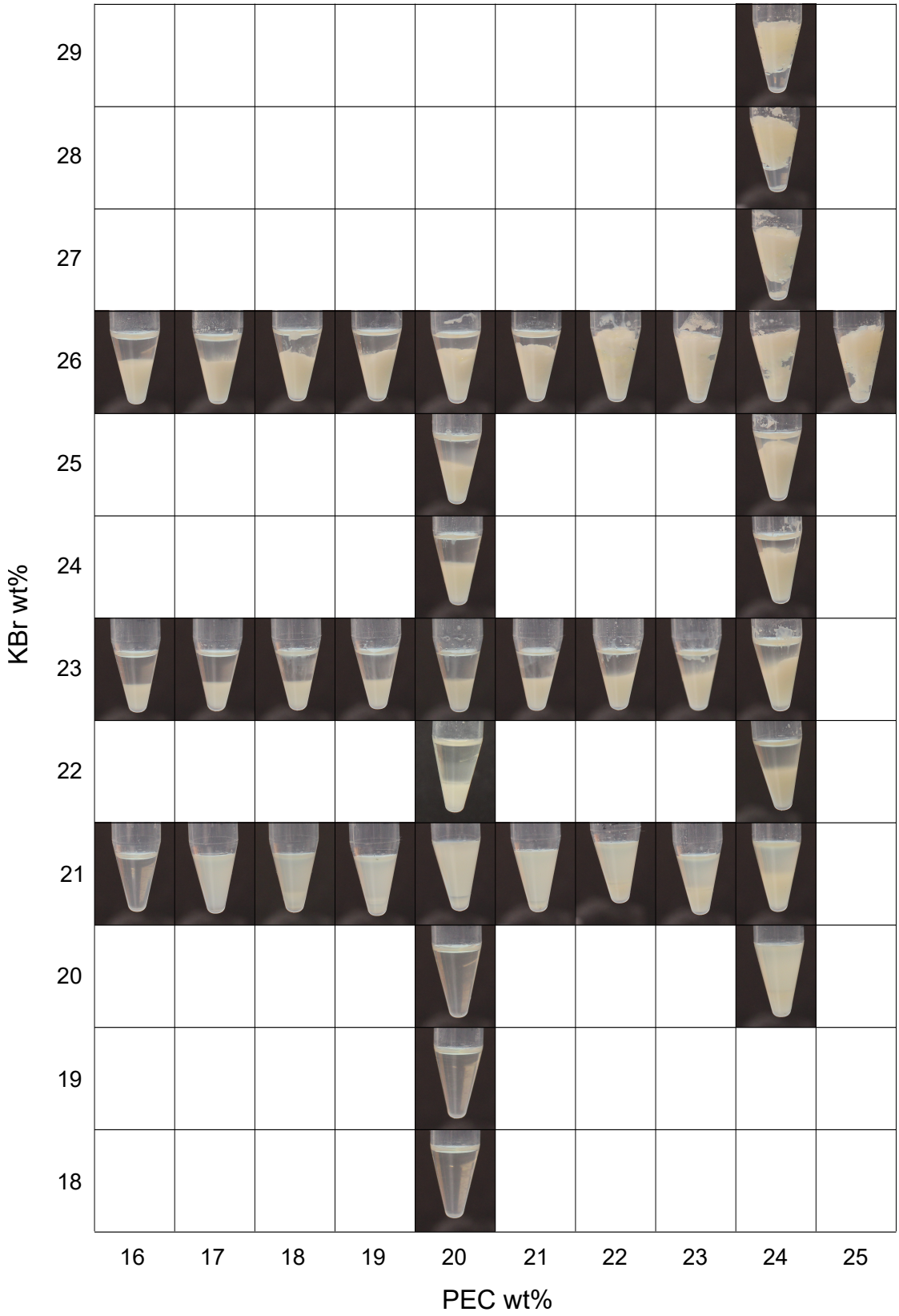

Figure S1. Photographs of samples prepared at high salt and polymer concentrations. Photos are labeled with the weight fractions of PEC and KBr at which each sample was prepared.

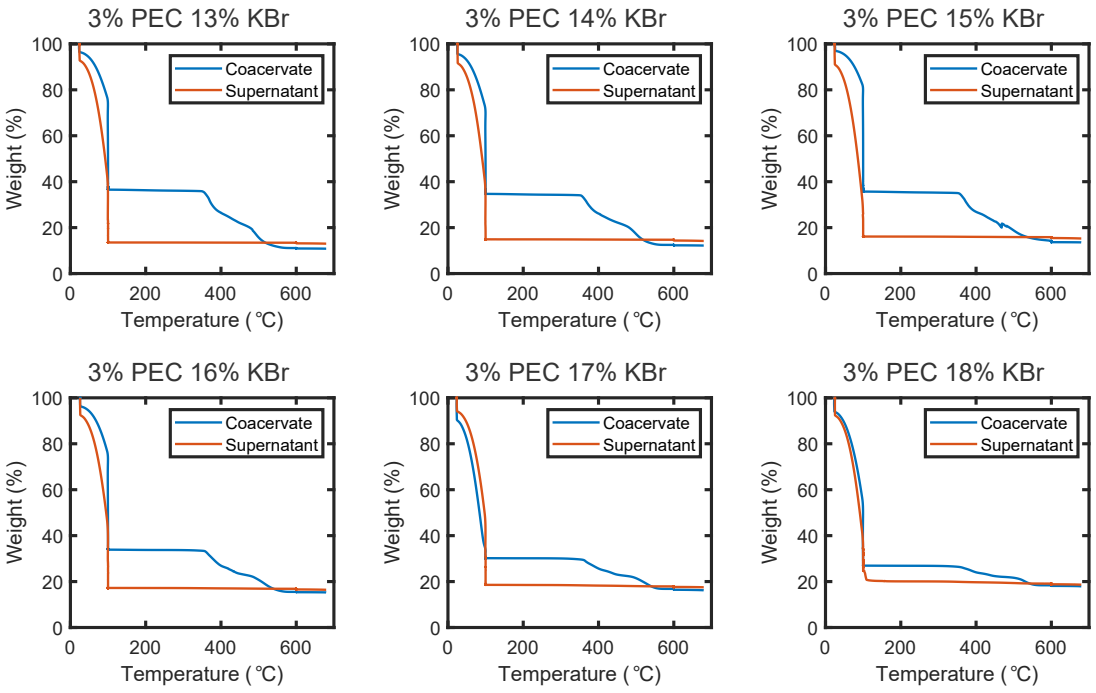

Figure S2. TGA traces of both phases of samples prepared under the binodal. The targeted weight fractions of PEC and KBr are listed above each panel.

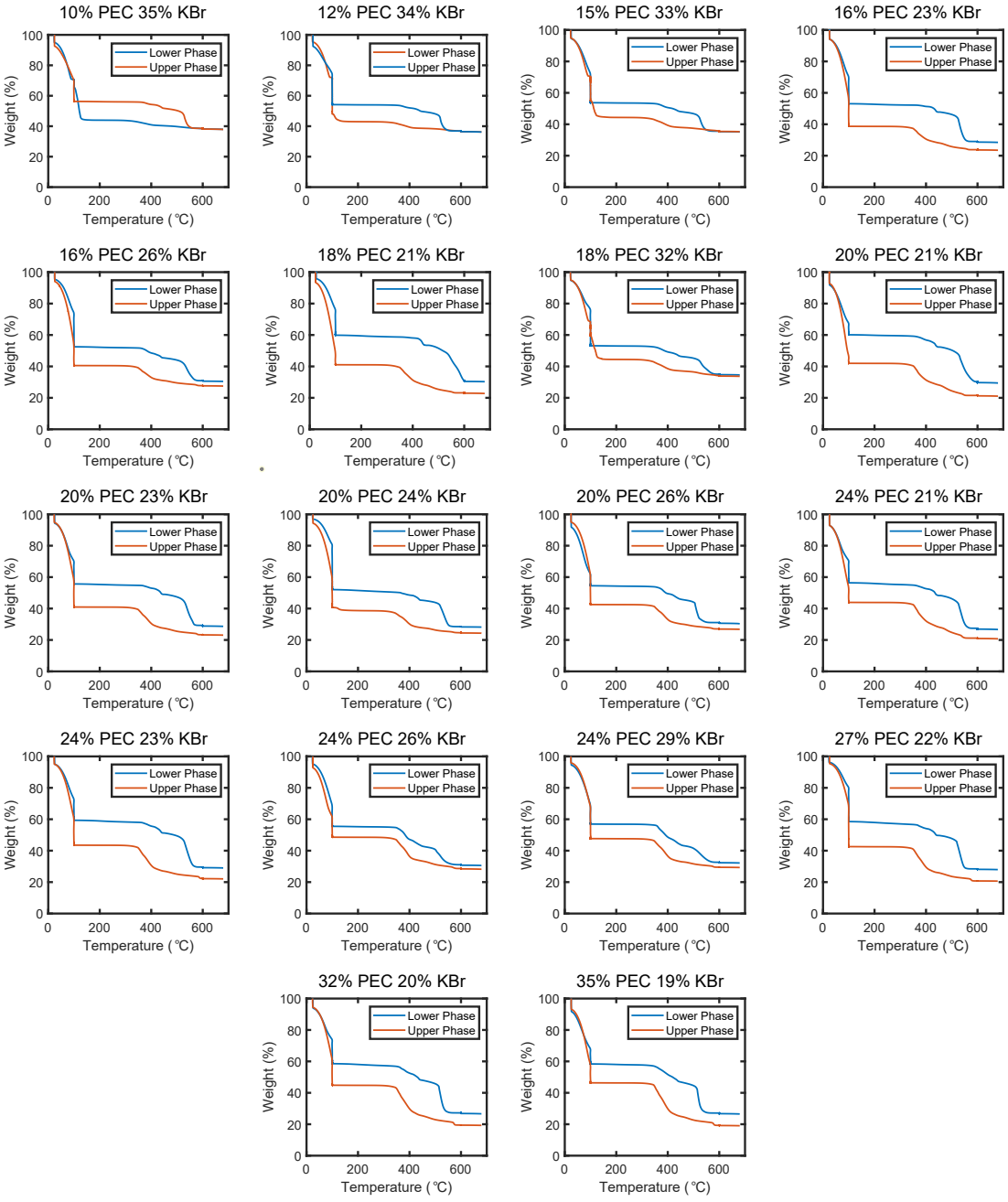

Figure S3. TGA traces of both phases of samples prepared in the UPW. The targeted weight fractions of PEC and KBr are listed above each panel.

TGA experiments were also carried out on samples of pure PSS^-K^+ (prepared by dialysis of PSS^-K^+ against KBr followed by milliQ water), pure $PDADMA^+Br^-$ (prepared by dialysis of $PDADMA^+Cl^-$ against KBr followed by milliQ water), and the salt-free PSS/PDADMA PEC used to prepare all samples. The resulting TGA traces are shown in Figure S4. As seen in this figure, the $PDADMA^+Br^-$ and PSS/PDADMA samples degraded completely by 600 °C under the conditions used for the TGA experiments. The PSS^-K^+, on the other hand, exhibited significant residue even at the highest temperatures (approximately 38% of the mass remained after the isotherm at 600 °C). This residual mass is consistent with degradation of PSS^-K^+ (chemical formula $C_8H_7O_3SK$, molecular weight 222.30 g/mol) to volatile products plus 0.5 eq. potassium sulfate (K_2SO_4, molecular weight 174.26 g/mol), although other inorganic byproducts (e.g. potassium sulfite) may also be present.

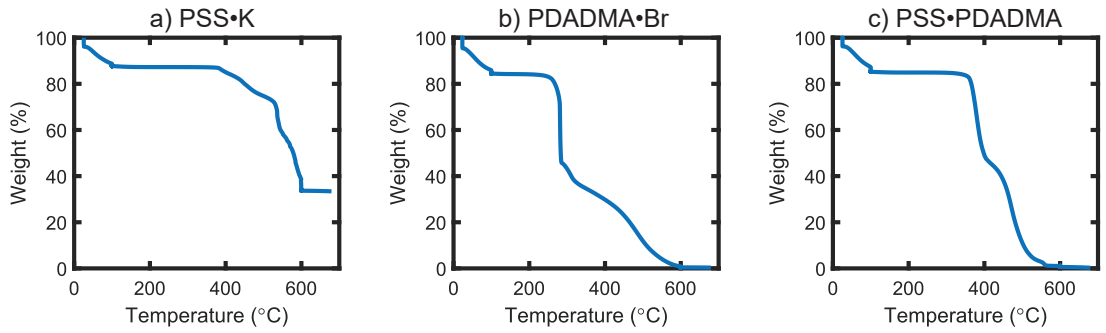

Figure S4. TGA traces of (a) PSS^-K^+, (b) $PDADMA^+Br^-$, and (c) salt-free PSS/PDADMA PEC. Samples were prepared from lyophilized, salt-free polymer samples; mass loss prior to 100 °C is attributed to loss of atmospheric water absorbed during sample preparation and transfer to the TGA pans.

S1.3 Nuclear Magnetic Resonance

Representative spectra of PSS, PDADMA, and a 1:1 stoichiometric PEC are shown in Fig. S5. In PSS, the protons from the aromatic rings appear between 6 and 8 ppm, and the protons from the backbone appear between 1 and 2 ppm. In PDADMA, the protons from the amine methyl groups appear between 3.3 and 3.8 ppm, the protons from the methylene units on the pyrrolidinium ring appear as two peaks of approximately equal intensity at 3.6 and 4.1 ppm, the protons from the

backbone methine appear as two peaks of unequal intensity at 2.6 and 2.9 ppm, and the protons from the backbone methylene units appear between 1.2 and 2 ppm. We note that the splitting of the pyrollidinium methylene and backbone methine peaks are often ignored in the literature, but are consistent with both the measured integrals and the expected splittings of protons on opposite faces of a substituted ring (for the pyrrolidinium methylenes) and the 6:1 cis:trans backbone stereochemistry previously reported for PDADMA (for the backbone methines).[1] The spectrum of the 1:1 PSS:PDADMA PEC, shown in Fig. S5(c), is essentially a linear combination of the individual PSS and PDADMA spectra, as expected. We note, however, that even though the number of PSS and PDADMA repeat units in the sample is the same, the peak intensity in the aliphatic region ($\delta < 4.5$ ppm) is significantly higher than the peak intensity in the aromatic region ($\delta \sim 6-8$ ppm) because of the large number of protons on each PDADMA repeat unit.

Spectra of all samples characterized in the UPW are shown in Figures S6-S8. In contrast to the spectrum of the stoichiometrically-balanced sample shown in Fig. S5(c), the ratios of the aromatic and aliphatic peaks vary widely, qualitatively indicating non-stoichiometric polymer partitioning.

As described in the main text, the stoichiometries of the individual phases were quantified from these spectra using

$$x_{PSS} = \frac{PSS}{PSS + PDADMA} = \frac{4I_{aromatic}}{4I_{aromatic} + (I_{aliphatic} - \frac{3}{4}I_{aromatic})} \tag{S1}$$

where $I_{aromatic}$ is the total intensity in the aromatic region (6-8 ppm) and I_{aliph} is the total intensity in the aliphatic region (1-4.5 ppm). This calculation, which is adapted from Shamoun et al.[2], is convenient because it does not require accounting for the splittings and overlaps of the peaks in the aliphatic region. However, with accurate assignment of the PDADMA spectrum, as described above, the mole fraction of PSS can also be calculated using

$$x_{PSS} = \frac{I_{aromatic}/4}{(I_{aromatic}/4 + I_{4.2}/2} \tag{S2}$$

where $I_{4.2}$ is the intensity of the peak at 4.2 ppm corresponding to half of the signal from the

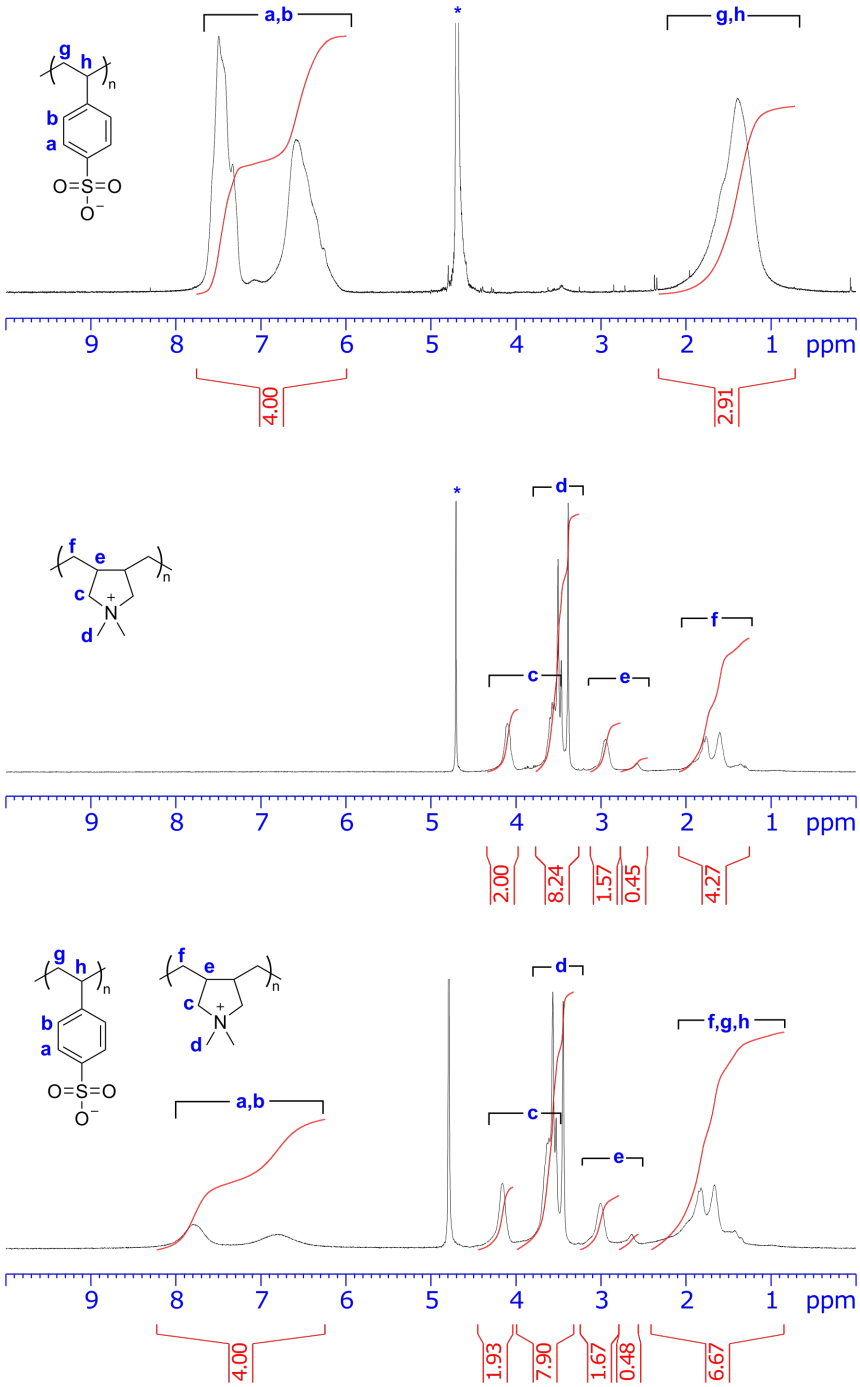

Figure S5. ^{1}H NMR spectra of (a) PSS, (b) PDADMA, and (c) a standard PEC composed of 1:1 PSS:PDADMA. In panel (c), analysis of the a,b and c peaks using equation S2 gives $x_{PSS} = 0.508$, while analysis of the total integrals of the aromatic and aliphatic regions using equation S1 gives $x_{PSS} = 0.506$.

pyrrolidinium methylenes. The integrals of the individual peaks used in these calculations, and the resulting values of x_{PSS}, are summarized in Table S1. As shown in this table, the x_{PSS} values

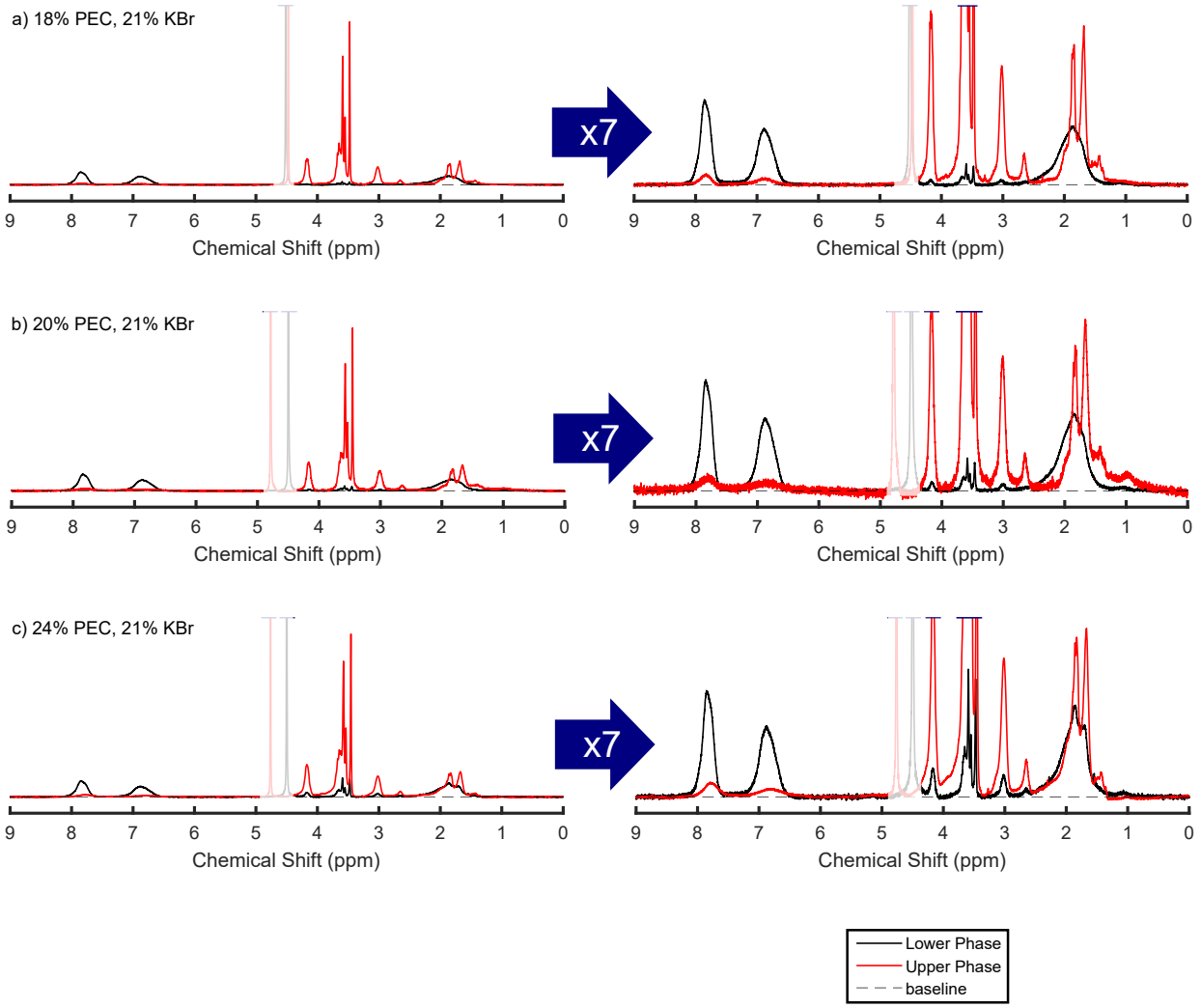

Figure S6. NMR spectra of both phases of samples prepared at 21 wt% KBr. The targeted weight fractions of PEC and KBr are listed above each figure. The left panel of each figure shows the full spectrum, while the right panel shows a 7x zoom. The baseline used for NMR integrals is indicated with a dashed line.

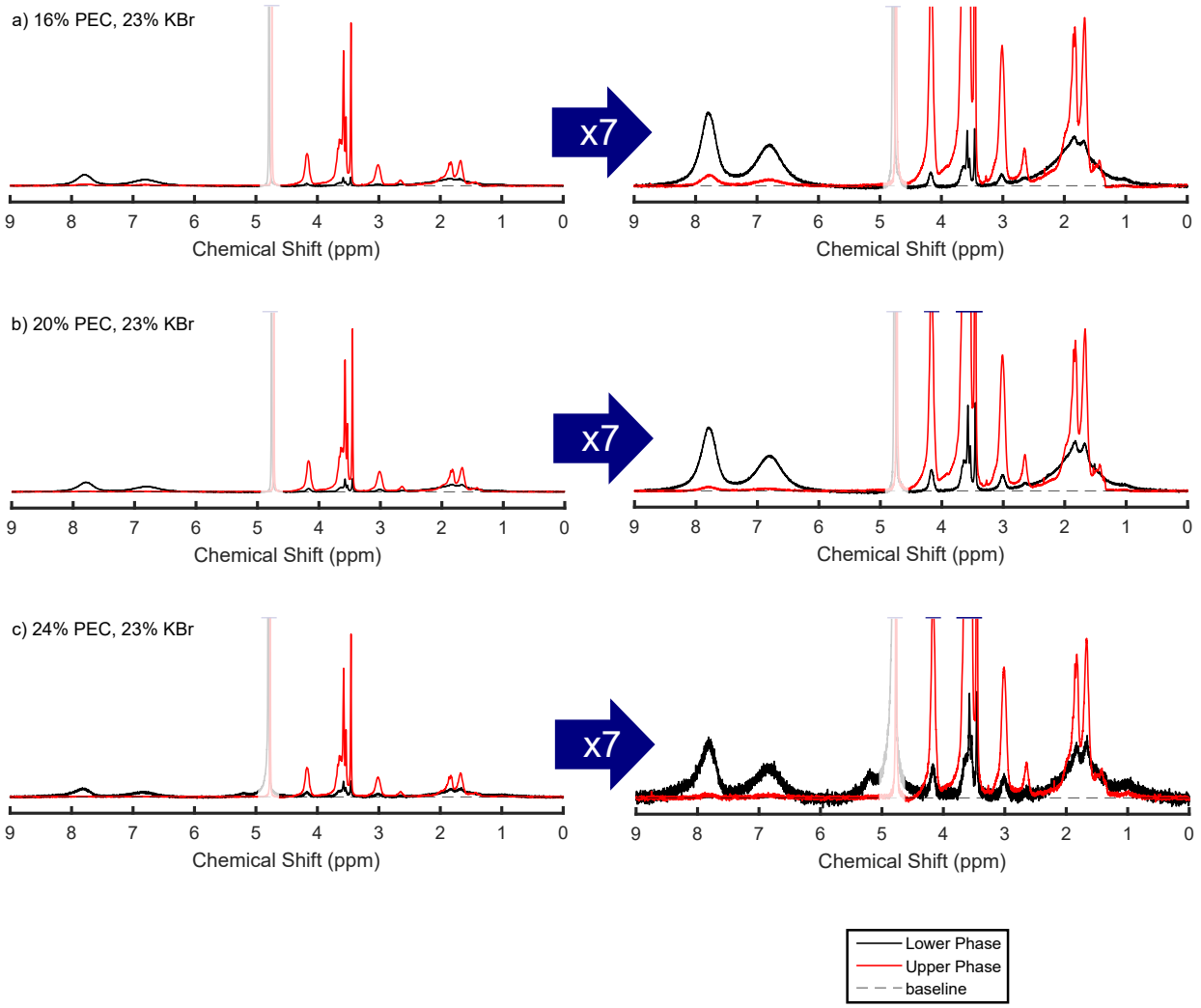

Figure S7. NMR spectra of both phases of samples prepared at 23 wt% KBr. The targeted weight fractions of PEC and KBr are listed above each figure. The left panel of each figure shows the full spectrum, while the right panel shows a 7x zoom. The baseline used for NMR integrals is indicated with a dashed line.

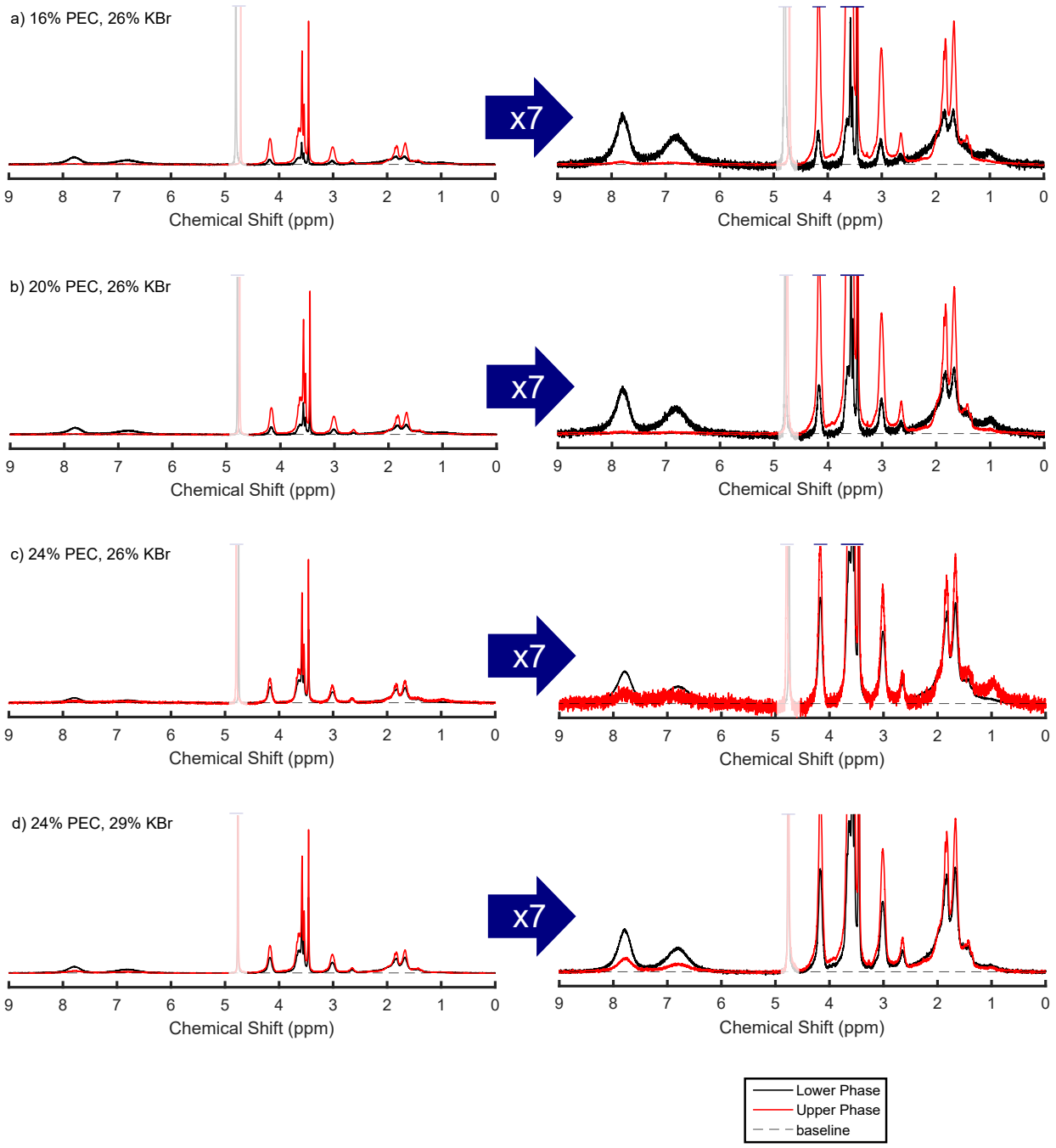

Figure S8. NMR spectra of both phases of samples prepared at 26 and 29 wt% KBr. The targeted weight fractions of PEC and KBr are listed above each figure. The left panel of each figure shows the full spectrum, while the right panel shows a 7x zoom. The baseline used for NMR integrals is indicated with a dashed line.

calculated by both methods agreed to within 5%. This variation is also consistent with the variation in x_{PSS} values between multiple independent measurements on the same sample, and 5% is thus used as the estimated error in the x_{PSS} values reported in this work.

Prepared Composition		Phase[a]	Integrals ($\times 10^{-3}$)					x_{PSS}	
PEC (wt%)	KBr (wt%)		6.4-8.2 ppm	4.0-4.3 ppm	3.3-3.8 ppm	2.5-3.2 ppm	0.8-2.5 ppm	Eq. S1	Eq. S2
18	21	L	135.7	1.6	7.4	4.3	106.2	0.969	0.977
		U	16.3	57.2	245.2	58.1	148.9	0.116	0.125
20	21	L	158.1	2.8	11.4	5.2	125.5	0.960	0.966
		U	5.9	10.7	49.0	12.3	33.9	0.189	0.216
24	21	L	105.5	6.0	27.3	8.0	95.3	0.880	0.898
		U	36.1	96.0	382.8	86.3	222.1	0.160	0.158
16	23	L	165.4	3.3	19.5	11.7	121.3	0.954	0.962
		U	28.1	94.4	378.9	87.5	217.7	0.130	0.130
20	23	L	179.2	8.1	39.7	16.1	143.5	0.908	0.917
		U	14.1	118.5	481.5	113.0	268.0	0.055	0.056
24	23	L	14.2	1.5	5.2	1.4	13.8	0.836	0.824
		U	4.4	38.4	161.0	37.9	93.2	0.051	0.054
16	26	L	21.2	1.7	9.1	2.5	22.0	0.814	0.862
		U	12.3	108.2	461.3	113.5	266.7	0.050	0.054
20	26	L	19.9	2.8	14.0	3.6	23.9	0.731	0.778
		U	5.7	73.1	312.1	76.1	178.8	0.035	0.038
24	26	L	141.7	64.4	276.0	71.7	237.9	0.489	0.506
		U	3.6	5.4	25.5	5.9	18.6	0.218	0.251
24	29	L	71.8	28.2	121.1	31.7	118.0	0.540	0.560
		U	31.5	65.0	271.0	66.2	172.3	0.187	0.196

[a] L = lower phase, U = upper phase

Table S1. Compositions of Phase-Separated Samples Obtained by ^{1}H-NMR

S1.4 Polymer Fraction

Plots of the polymer fraction in each sample, analogous the those for the mole fraction of PSS presented in Figures 6 and 7 in the main text, are presented in Figs. S9-S10.

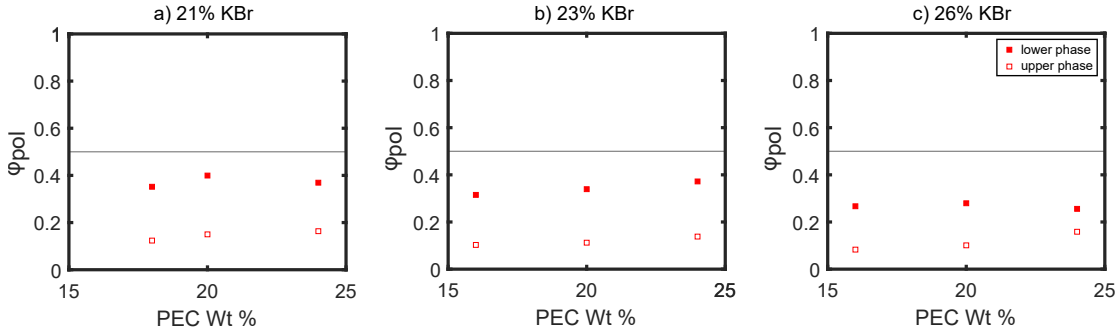

Figure S9. Volume fraction of polymer in the dense (filled squares) and dilute (open squares) phases of samples prepared with (a) 21%, (b) 23%, and (c) 26% KBr by weight.

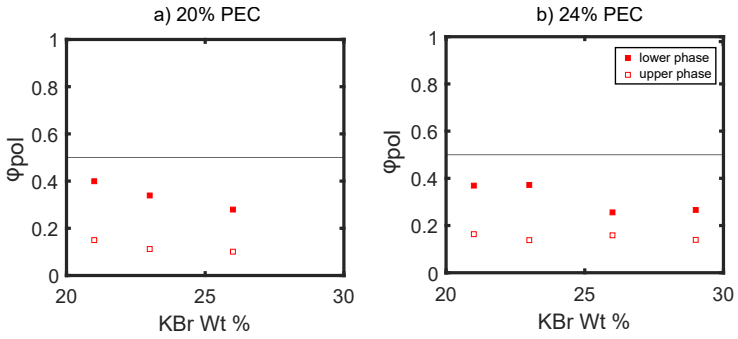

Figure S10. Volume fraction of polymer in the dense (filled squares) and dilute (open squares) phases of samples prepared with (a) 20% and (b) 24% PEC by weight.

S1.5 Infrared Spectroscopy

As noted in the main text, the TGA analysis suggested that PSS and PDADMA partition into different phases in the UPW. While ^{1}H NMR was used as the primary method for quantifying this partitioning, ATR-FTIR measurements were also performed to (1) provide further evidence for segregative phase separation and (2) determine whether there are are significant differences in the polymer hydration in these two phases. Representative IR spectra of the upper and lower phases

of a sample prepared in the UPW are shown in Figure S11. This spectrum exhibits a number of distinct features that are attributable to different molecular species in the sample. The peaks between 3700-2700 cm^{-1} and 1800-1600 cm^{-1} correspond to the stretching and bending modes of water, respectively. The peaks at 1450 and 1400 cm^{-1} correspond to the C-H stretching of the methyl group and C-N stretching modes of PDADMA, and the peaks at 1100 and 1000 cm^{-1} correspond to the C=C and S=O stretching modes of PSS. The shape of the peak corresponding to the water stretching mode between 3700 and 2700 cm^{-1} gives information about perturbation of the hydrogen-bonding network in the solvent. In both the upper and lower phases, this peak is narrower and somewhat blue-shifted compared to that of bulk water, indicating disruption of hydrogen bonds to accommodate the high polymer and salt concentrations[3]. The shape of this peak is similar for both the upper and lower phases, indicating that their hydration environments are comparable. As expected from the NMR measurements, however, the relative intensities of the peaks corresponding to PSS and PDADMA differed between the two phases. The peaks arising from PSS had a significantly stronger absorbance in the lower, polymer-rich phase, while the peaks arising from PDADMA had a slightly stronger absorbance in the upper phase. Spectra of other samples prepared in the UPW exhibited similar trends (Fig. S12). These results are qualitatively consistent with the partitioning observed by NMR, and provide further evidence for the occurence of segregative phase separation at high salt concentrations.

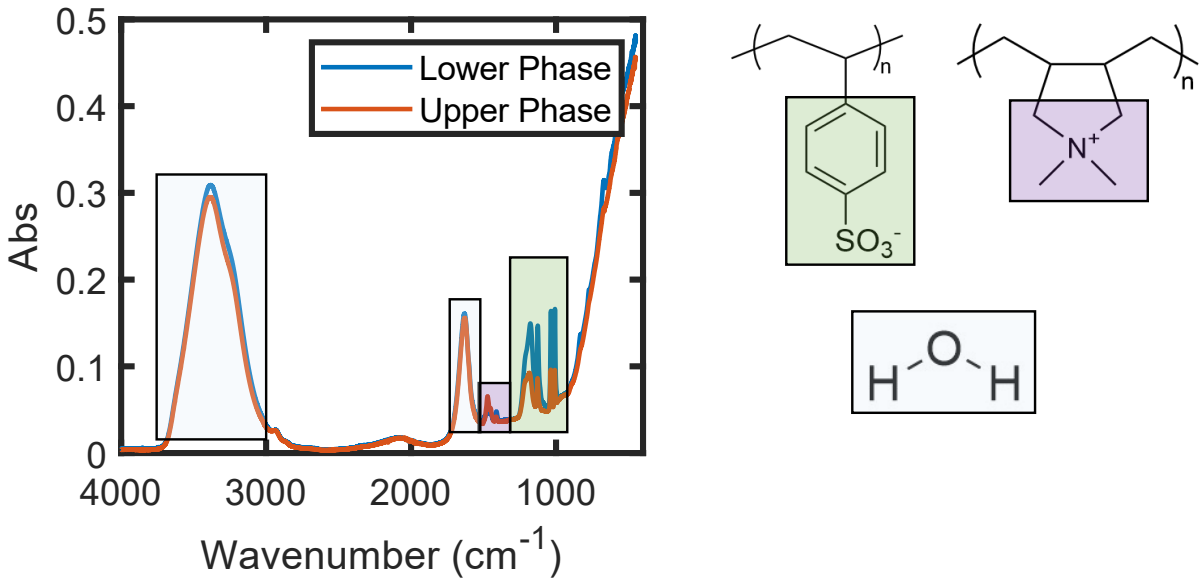

Figure S11. ATR-FTIR spectra of the lower and upper phases of a sample prepared at KBR and PEC concentrations of 21% and 20% KBr, respectively, with assignments of vibrational modes for each major peak in the spectrum.

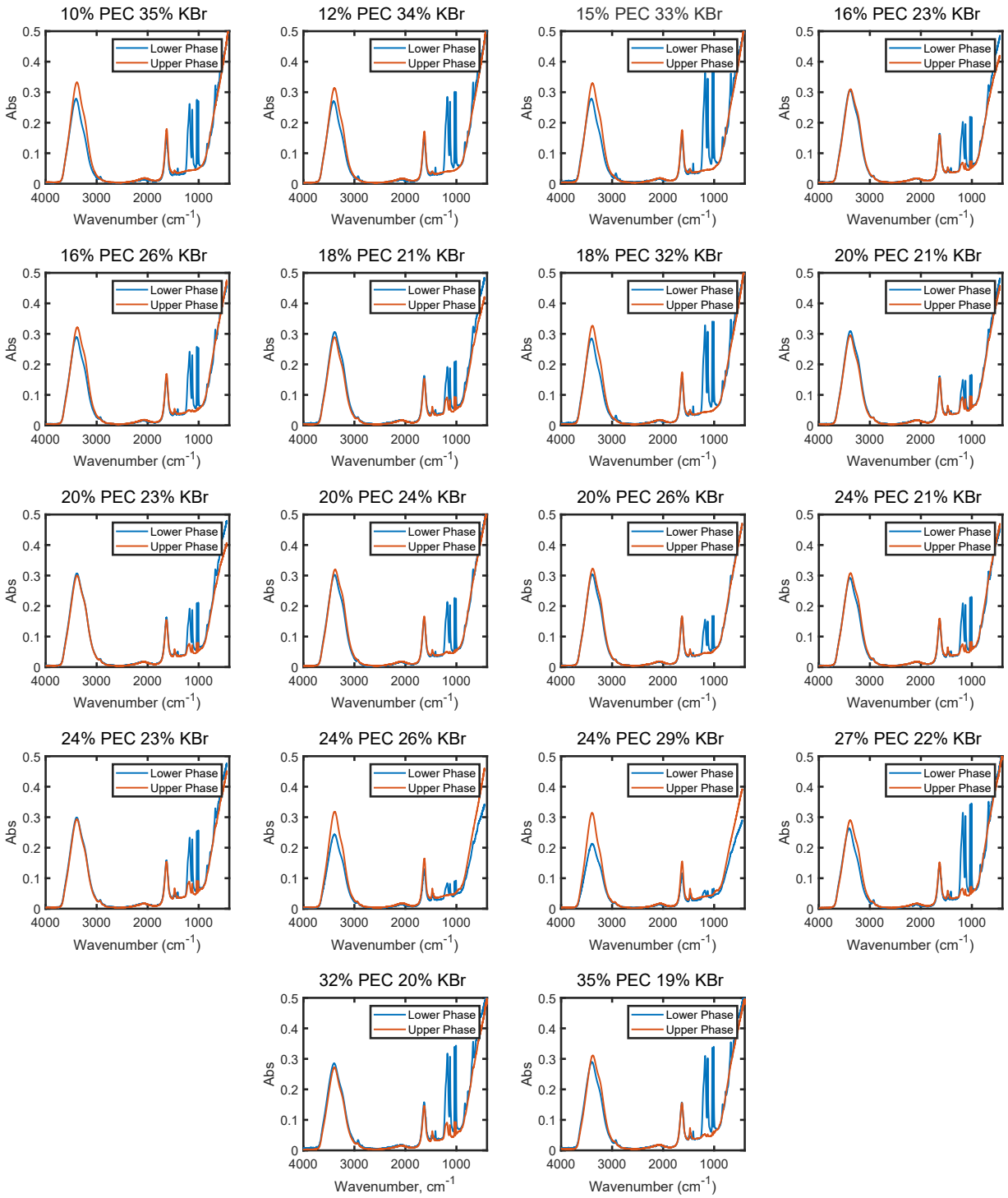

Figure S12. ATR-FTIR spectra of both phases of samples prepared in the UPW. The targeted weight fractions of PEC and KBr are listed above each figure.

S1.6 High-Salt Phase Behavior of PSPSA/PDADMA

As noted in the main text, a small number of experiments were also carried out on complexes of poly(sulfopropyl acrylate) (PSPA, $M_n \approx 200,000$ g/mol, Sigma-Aldrich) and poly(diallyldimethylammonium) (PDADMA, $M_w \approx 200,000 - 350,000$ g/mol, Sigma-Aldrich) in the presence of sodium chloride to determine whether phase separation in the UPW is unique to the PSS/PDADMA system or whether it is a more general phenomenon of strong polyelectrolytes. Samples were prepared using the same method as described for the $PSS^-PDADMA^+$ samples described in the main text. Photographs of samples prepared with PEC fractions of approximately 24 wt% and salt fractions between 14 and 23 wt% are shown in Figure S13. As seen in this figure, the PSPA/PDADMA system phase separated at salt concentrations above approximately 19 wt%, far above the binodal for this system. Interestingly, at the highest salt concentrations, a solid that appeared to be crystalline NaCl was also observed at the bottom of the dense phase, suggesting that NaCl actually becomes insoluble in the polymer solution at these high concentrations.

TGA traces for representative phase-separated samples prepared at both low and high salt concentrations are shown in Figure S14. As in the PSS/PDADMA system, samples prepared at low salt concentrations (underneath the conventional binodal) phase separated into a polymer-rich and a polymer-poor phase, while samples that phase separated at high salt concentrations contained significant polymer content in both phases. Finally, ATR-FTIR spectra of the upper and lower phases of the sample prepared at high salt concentrations, shown in Figure S15, indicated that the polymers also partitioned between the phases in a non-stoichiometric fashion, with the PSPA found primarily in the lower, denser-phase and the PDADMA found primarily in the upper, less-dense phase. Qualitatively, these trends match those observed in the PSS/PDADMA system, indicating that phase-separation in the UPW is a more general phenomenon of strong polyelectrolyte systems and is not restricted to aromatic polymers.

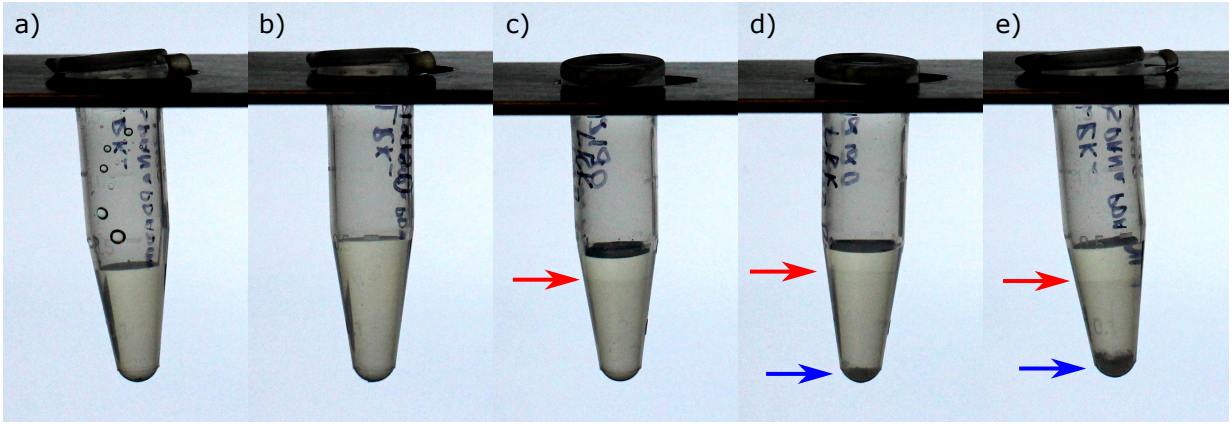

Figure S13. Photographs of PSS/PDADMA samples prepared with overall polymer fractions of 24 ± 1 wt% and NaCl fractions of (a) 14.4 wt%, (b) 16.4 wt%, (c) 19.3 wt%, (d) 21.3 wt%, and (e) 23.1 wt%. Red arrows indicate the boundary between the upper and lower liquid phases, while blue arrows indicate solid NaCl that did not dissolve at the highest salt concentrations.

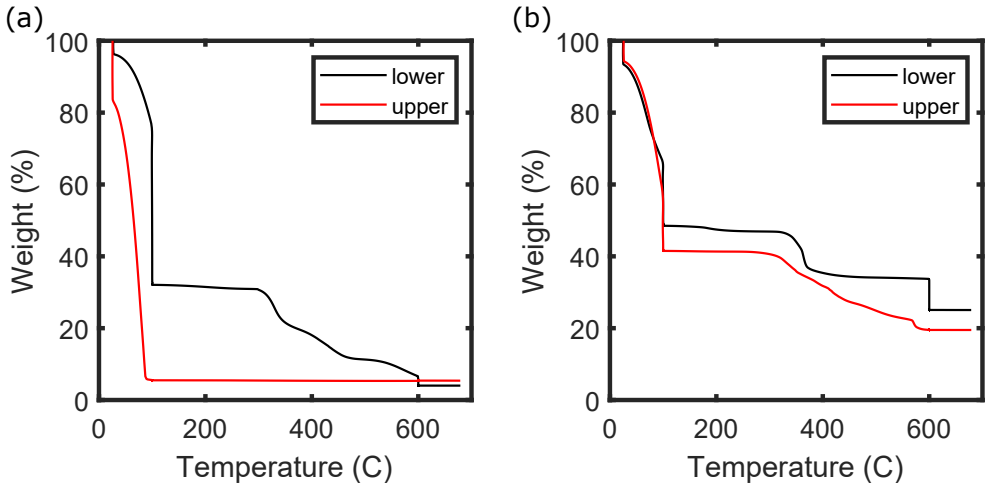

Figure S14. TGA traces of the upper and lower phases of PSPA/PDADMA samples prepared (a) at low salt and low polymer concentrations (0.1 M polymer and 0.8 M NaCl) and (b) high salt and high polymer concentrations (approx. 21.9 wt% polymer and 25.0 wt% NaCl).

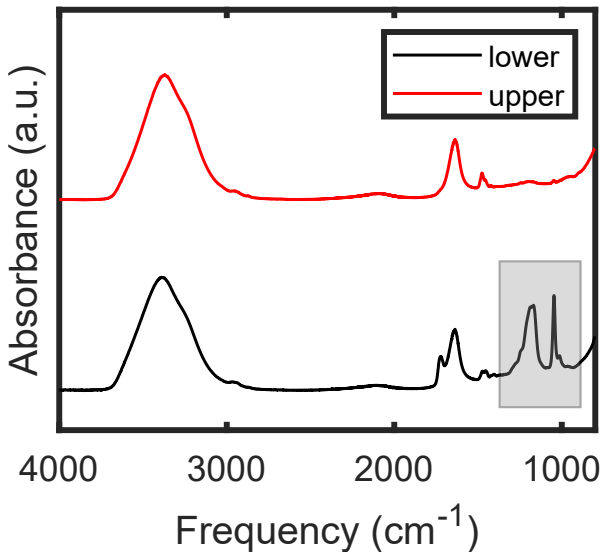

Figure S15. ATR-FTIR spectra of the upper and lower phases of a PSPA/PDADMA sample prepared at high salt and high polymer concentrations (approx. 21.9 wt% polymer and 25.0 wt% NaCl). The lower phase contains characteristic signatures of the sulfonate group (highlighted), while the upper phase does not.

S2 Supplemental Analysis

S2.1 Correction of TGA for Non-Stoichiometric Samples

As shown in Figure S4, samples of both $PDADMA^+Br^-$ and stoichiometric PDADMA/PSS complexes degrade completely before 600 °C in TGA experiments. Samples of PSS^-K^+, on the other hand, leave behind substantial residual mass at temperatures up to 700 °C, which we attribute to formation of non-volatile salts such as KSO_3 and K_2SO_4. As such, the mass loss between 100-600°C and the residual mass retained between 600-800 °C do *not* map directly onto the weight fractions of polymer and salt in the material, especially for samples containing excess PSS, and the TGA data for stoichiometrically-imbalanced samples must be corrected to obtain the true mass fractions of the organic and inorganic components prior to construction of the phase diagram.

This correction was performed as follows.

First, for each sample, we denote the *measured* mass loss at low temperatures (below 100 °C) as w_{low}, that at intermediate temperatures (100-600 °C) as w_{med}, and that at high temperatures

(>600 °C) as w_{high}. These values are *known*, or obtained directly from the TGA experiments. The *actual* mass fractions of water, PSS^-, $PDADMA^+$, K^+, and Br^- in the sample are denoted w_{H_2O}, w_{PSS}, w_{PDADMA}, w_K, and w_{Br}, respectively; these values are *unknown* and need to be determined from the analysis. Assuming that the mass loss below 100°C is attributable only to water, i.e.

$$w_{H_2O} = w_{low} \tag{S3}$$

this leaves four unknown values, requiring four constraint equations to uniquely determine their values.

For all samples, the first constraint arises from the requirement that the sample must be charge neutral. This constraint is expressed as

$$n_{PSS} + n_{Br} = n_{PDADMA} + n_K \tag{S4}$$

where n_{PSS}, n_{PDADMA}, n_{Br}, and n_K are the number of moles of PSS^- and $PDADMA^+$ repeat units and Br^- and K^+ ions, respectively. Written in terms of the weight fractions (which we interpret here as the mass of each species present in 1 g of sample), this constraint becomes

$$\frac{w_{PSS}}{m_{PSS}} + \frac{w_{Br}}{m_{Br}} = \frac{w_{PDADMA}}{m_{PDADMA}} + \frac{w_K}{m_K} \tag{S5}$$

where $m_{PSS} = 184.2$ g/mol, $m_{PDADMA} = 126.2$ g/mol, $m_{Br} = 79.9$ g/mol, and $m_K = 39.1$ g/mol are the molar masses of individual PSS^- and $PDADMA^+$ repeat units and Br^- and K^+ ions, respectively.

The second constraint for all samples is obtained from the PSS/PDADMA stoichiometry measured by NMR. The mole fraction of PSS in the organic component is given by

$$x_{PSS,PEC} = \frac{n_{PSS}}{n_{PSS} + n_{PDADMA}} \tag{S6}$$

or, in terms of weight fractions,

$$x_{PSS,PEC} = \frac{\frac{w_{PSS}}{m_{PSS}}}{\frac{w_{PSS}}{m_{PSS}} + \frac{w_{PDADMA}}{m_{PDADMA}}} \tag{S7}$$

The third and fourth constraints differ for samples with excess PDADMA and those with excess PSS.

For samples with excess PDADMA, since both stoichiometric $PSS^-PDADMA^+$ complexes and $PDADMA^+Br^-$ degrade completely below 600 °C, the mass loss between 100 and 600 °C corresponds to the mass of the stoichiometric portion of the $PSS^-PDADMA^+$ complex plus the mass of the stoichometric excess of $PDADMA^+Br^-$ (or, the mass of all of the the PSS^- and $PDADMA^+$, plus the mass of the Br^- ions associated with the excess $PDADMA^+$). This gives rise to the constraint

$$w_{med} = w_{PSS} + w_{PDADMA} + m_{Br}(n_{PDADMA} - n_{PSS}) \tag{S8}$$

$$= w_{PSS} + w_{PDADMA} + m_{Br}\left(\frac{w_{PDADMA}}{m_{PDADMA}} - \frac{w_{PSS}}{m_{PSS}}\right) \tag{S9}$$

The remaining mass above 600 °C then corresponds to the mass of the stoichiometric portion of the KBr (or, the total mass of K^+ and Br^- less the mass of the Br^- ions lost with the excess $PDADMA^+$), giving rise to the constraint

$$w_{high} = w_K + w_{Br} - m_{Br}(n_{PDADMA} - n_{PSS}) \tag{S10}$$

$$= w_K + w_{Br} - m_{Br}\left(\frac{w_{PDADMA}}{m_{PDADMA}} - \frac{w_{PSS}}{m_{PSS}}\right) \tag{S11}$$

Rearranging equations S5, S7, S9, and S11 yields the following system of four equations with four unknowns, which can be solved using appropriate numerical computing packages to obtain

the desired mass fractions of PSS^-, $PDADMA^+$, Br^-, and K^+ for each sample:

$$\begin{pmatrix} \frac{1}{m_{PSS}} & \frac{-1}{m_{PDADMA}} & \frac{-1}{m_K} & \frac{1}{m_{Br}} \\ \frac{x_{PSS,PEC}-1}{m_{PSS}} & \frac{x_{PSS,PEC}}{m_{PDADMA}} & 0 & 0 \\ 1-\frac{m_{Br}}{m_{PSS}} & 1+\frac{m_{Br}}{m_{PDADMA}} & 0 & 0 \\ \frac{m_{Br}}{m_{PSS}} & \frac{-m_{Br}}{m_{PDADMA}} & 1 & 1 \end{pmatrix} \begin{pmatrix} w_{PSS} \\ w_{PDADMA} \\ w_K \\ w_{Br} \end{pmatrix} = \begin{pmatrix} 0 \\ 0 \\ w_{med} \\ w_{high} \end{pmatrix} \tag{S12}$$

As shown in Fig. S4(a), samples containing only PSS^-K^+ lose approximately 60% of their non-water mass in the 100-600 °C range and the remaining 40% of their non-water mass in the 600-800 °C range. For mixed samples with excess PSS^-K^+, the mass loss in the 100-600°C range is thus the mass of the stoichiometric portion of the PEC plus 60% of the mass of the excess PSS^-K^+, while the mass loss in the 600-800 °C range is the mass of the stoichiometric portion of the KBr plus the remaining 40% of the mass of the excess PSS^-K^+. These constraints are expressed as

$$w_{med} = w_{PDADMA} + m_{PSS} n_{PDADMA} + f(m_{PSS}+m_K)(n_{PSS}-n_{PDADMA}) \tag{S13}$$

$$= w_{PDADMA} + m_{PSS}\frac{w_{PDADMA}}{m_{PDADMA}} + f(m_{PSS}+m_K)(\frac{w_{PSS}}{m_{PSS}} - \frac{w_{PDADMA}}{m_{PDADMA}}) \tag{S14}$$

and

$$w_{high} = w_{Br} + m_K n_{Br} + (1-f)(m_{PSS}+m_K)(n_{PSS}-n_{PDADMA}) \tag{S15}$$

$$= w_{Br} + m_K\frac{w_{Br}}{m_{Br}} + (1-f)(m_{PSS}+m_K)(\frac{w_{PSS}}{m_{PSS}} - \frac{w_{PDADMA}}{m_{PDADMA}}) \tag{S16}$$

where f is the fraction of the mass of excess PSS^-K^+ lost in the 100-600°C range ($f \approx 0.6$).

As in the excess PDADMA case, rearranging equations S5, S7, S14, and S16 yields the following system of four equations with four unknowns, which can be solved using appropriate numerical computing packages to obtain the desired mass fractions of PSS^-, $PDADMA^+$, Br^-, and K^+ for each sample:

$$\begin{pmatrix} \frac{1}{m_{PSS}} & \frac{-1}{m_{PDADMA}} & \frac{-1}{m_K} & \frac{1}{m_{Br}} \\ \frac{x_{PSS,PEC}-1}{m_{PSS}} & \frac{x_{PSS,PEC}}{m_{PDADMA}} & 0 & 0 \\ \frac{f(m_{PSS}+m_K)}{m_{PSS}} & 1+\frac{m_{PSS}-f(m_{PSS}+m_K)}{m_{PDADMA}} & 0 & 0 \\ \frac{(1-f)(m_{PSS}+m_K)}{m_{PSS}} & \frac{-(1-f)(m_{PSS}+m_K)}{m_{PDADMA}} & 0 & 1+\frac{m_K}{m_{Br}} \end{pmatrix} \begin{pmatrix} w_{PSS} \\ w_{PDADMA} \\ w_K \\ w_{Br} \end{pmatrix} = \begin{pmatrix} 0 \\ 0 \\ w_{med} \\ w_{high} \end{pmatrix} \quad \text{(S17)}$$

References

[1] J. E. Lancaster, L. Baccei and H. P. Panzer, *Journal of Polymer Science: Polymer Letters Edition*, 1976, **14**, 549–554.

[2] R. F. Shamoun, H. H. Hariri, R. A. Ghostine and J. B. Schlenoff, *Macromolecules*, 2012, **45**, 9759–9767.

[3] C. I. Eneh, M. J. Bolen, P. C. Suarez-Martinez, A. L. Bachmann, T. J. Zimudzi, M. A. Hickner, P. Batys, M. Sammalkorpi and J. L. Lutkenhaus, *Soft Matter*, 2020, **16**, 2291–2300.